INTERNAL RESPONSE OF CATCHMENT TO PLAUSIBLE PARAMETER SETS UNDER EQUIFINALITY

Giha LEE [1], Yasuto TACHIKAWA[2], Takahiro SAYAMA[3] and Kaoru TAKARA[4]

[1]Student Member, Graduate student, Dept. of Urban and Environmental Eng., Kyoto University (Nishikyo-ku, Kyoto 615-8540, Japan)

[2]Member of JSCE, Dr. Eng., Associate Professor, Dept. of Urban and Environmental Eng., Kyoto University (Nishikyo-ku, Kyoto 615-8540, Japan)

[3]Member of JSCE, Dr. Eng., Assistant Professor, DPRI, Kyoto University (Gokasho, Uji 611-0011, Japan)

[4]Fellow of JSCE, Dr. Eng., Professor, DPRI, Kyoto University (Gokasho, Uji 611-0011, Japan)

A natural rainfall-runoff process is conceptualized by means of mathematical form reflecting a physical law and hydrologist's perception and it is typically calibrated and verified based on streamflow data, the commonly used catchment response. The streamflow data is obviously required, but is not sufficient to identify a conceptual parameter of a hydrologic model since numerous parameter combinations can often result in quite similar numerical values in terms of objective function and even indistinguishable simulated hydrographs. One of the efficient techniques to resolve this impasse is a combination of the model with streamflow data augmented by other kinds of hydrological information relevant to the prediction. In this study, internal dynamic response of catchment, spatiotemporally separated components of hydrograph, to the various mimic parameter sets is presented. It is concluded that all of simulations based on plausible parameter combinations sampled by using deterministic and stochastic automatic optimization algorithms, are performed equally well in terms of both model performance measure and visual comparison between observed and simulated hydrograph while internal behaviors of catchment show totally different aspects. The spatiotemporal information presented here can be utilized as one of the complementary constraints capable of filtering out non-physical parameter set(s).

Key Words: *plausible parameter sets, complementary constraint, internal dynamic response*

1. INTRODUCTION

One of significant steps in a rainfall-runoff modeling is parameter estimation, typically referred to as calibration. However, despite a remarkable improvement of automatic optimization algorithms, uncertainty in the calibrated parameter estimates still remains very large since a large number of different parameter sets can, in many cases, result in identical measures of model performance and even indistinguishable streamflow sequences[1),2)]. Beven and Binley[3)] used the special term 'equifinality' to explain the possibility of plausible parameter sets and it has been an interesting major issue in complicated hydrological modeling.

A rainfall-runoff model is mostly identified based on streamflow. Kuczera and Franks[4)] argued that it is obviously required, but is not sufficient information to identify the conceptual model parameter(s). An effective technique to resolve this insufficiency is to increase the amount of information through the use of additional output variables such as runoff, soil moisture, piezometric levels measured at different locations within the catchment, environmental isotopes and so on[5)] and then combine the runoff model with streamflow data augmented by those hydrological variables.

The additional information may be attractive for further conditioning or testing of a hydrologic model, but on the other hand, the utilization of this auxiliary information often requires additional model complexity in terms of reformulation of model equations due to adding auxiliary assumption and parameter. It means that this complementary information is likely to cause over-complexity of the model and as a result, it precludes falsification of unsuitable parameter combinations[4),6)]. Therefore, it is worthwhile developing a way to test models more comprehensively and incisively, given inherent limitations of the available streamflow data without increasing model complexity[7)].

Experimental methods such as isotope tracers, isotopic hydrograph separations and stream water residence time have been useful to provide additional evaluative criteria for water quantity and quality modeling. However, as noted above, these approaches, to some degree, require the revision of model for producing multiple output variables so that it again results in declination of parameter identifiability. To avoid this dilemma, Sayama *et al.*[8] proposed a hydrograph separation method derived from a spatiotemporal record matrix of streamflow and combined this scheme with a nonlinear distributed model that takes into account unsaturated, saturated subsurface and surface flow. This method can temporally split the hydrograph into the same number of corresponding components to the selected number of rainfall segments without any hydrochemical measure. Moreover, it can track the spatial origin of streamflow at a specific time step and then visualize the distributed runoff sources. Consequently, this new technique enables to analyze the effect of mimic parameter combinations on internal response to both pre-event and event in a catchment and then to be utilized as a posteriori evaluative benchmark to reject erroneous parameter combination(s).

In this study, we aim to exemplify both the presence of mimic parameter sets and the limitation of streamflow data for model identification and then we propose complementary information, internal behavior of catchment, capable of filtering out unreliable parameter sets from numerous plausible ones. This additional constraint is obtained from the spatiotemporal record matrix of streamflow[8].

2. APPLIED DISTRIBUTED RAINFALL-RUNOFF MODEL, OHDIS-KWMSS

OHymos based DIstributed hydrologic model with Kinematic Wave Method for Surface and Subsurface runoff (OHDIS-KWMSS) assumes that a permeable soil layer covers the hillslope as illustrated in **Fig. 1**. The soil layer consists of a capillary layer in which unsaturated flow occurs and a non-capillary layer where saturated flow occurs. According to this runoff mechanism, if the depth of water, h is higher than the soil depth, D then overland flow occurs.

The stage-discharge relationship[9] is defined as:

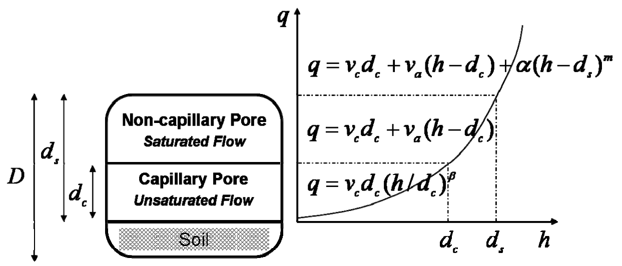

Fig. 1 Schematic model structure and extended stage-discharge relationship of OHDIS-KWMSS.

$$q = \begin{cases} v_c d_c (h/d_c)^\beta, & 0 \le h \le d_c \\ v_c d_c + v_a(h-d_c), & d_c \le h \le d_s \\ v_c d_c + v_a(h-d_c) + \alpha(h-d_s)^m, & d_s \le h \end{cases} \tag{1}$$

$$\frac{\partial h}{\partial t} + \frac{\partial q}{\partial x} = r(t) \tag{2}$$

Flow rate, q of each slope segment is calculated by above governing equations combined with the continuity equation (2), where $v_c = k_c i$; $v_a = k_a i$; $k_c = k_a / \beta$; $\alpha = \sqrt{i}/n$; i is slope gradient, k_c is hydraulic conductivity of the capillary soil layer, k_a is hydraulic conductivity of the non-capillary soil layer, n is roughness coefficient, the water depth corresponding to the water content is d_s and the water depth corresponding to maximum water content in the capillary pore is d_c. There are five parameters (n, k_a, d_s, d_c and β), which are assumed to have homogeneous values spatially, to be optimized in OHDIS-KWMSS.

3. PLAUSIBLE PARAMETER SETS

In this study, seven different parameter sets are prepared to investigate the influence of those on overall and internal model performances. First three parameter sets are estimated by deterministic automatic optimization algorithm, Shuffled Complex Evolution (SCE) method[1] with three different Objective Functions (OFs), SLS, HMLE and MIA (refer to Lee *et al.*[10] for more details about OFs). Secondly, the optimal value tuned by stochastic optimization algorithm, Shuffled Complex Evolution Metropolis (SCEM) method[11] is also utilized (*i.e.* OPT, approximately near the highest densities in each posterior parameter distribution estimated by SCEM). Finally, other three remainders are randomly sampled from the estimated posterior parameter distribution based on different events (*i.e.* Sample (1), (2) and (3)). **Table 1** summarizes all parameter values used here and **Fig. 2** presents both the marginal posterior probability distributions for the each parameter of OHDIS-KWMSS, obtained using behavioral 6000 parameter sets after the SCEM implementation, and the optimal values of chosen parameter sets.

Table 1 Selected plausible parameter sets.

	n [m$^{-1/3}$ s]	k_a [m/s]	d_s [m]	d_c [m]	β [-]
SLS	0.5	0.013	0.893	0.496	19.8
HMLE	0.5	0.011	0.485	0.085	2.95
MIA	0.5	0.010	0.468	0.068	2.59
OPT	0.5	0.013	0.865	0.472	18.6
Sample(1)	0.49	0.049	0.510	0.480	2.95
Sample(2)	0.5	0.050	0.610	0.430	4.47
Sample(3)	0.5	0.019	0.619	0.468	6.20

4. CONCEPT OF HYDROGRAPH SEPARARATION METHOD

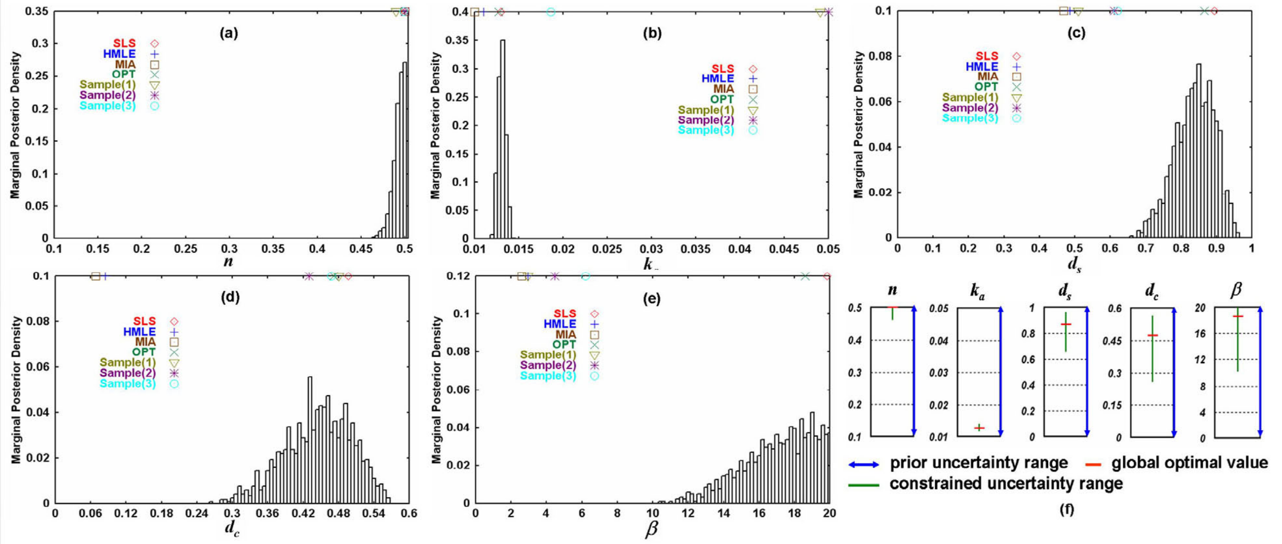

Fig. 2 (a) ~ (e) Marginal posterior parameter probability distributions of the OHDIS-KWMSS and the selected plausible parameter sets marked in upper horizontal axes and (f) Initial and constrained parameter uncertainty ranges.

The concept of hydrograph separation method[8)] based on spatiotemporal record of streamflow is presented in **Fig. 3**(a), (b). **Fig. 3**(a) illustrates the temporally separated hydrograph in regard of five rainfall durations (0~4) within a single event. Herein, 0 hydrograph component in **Fig. 3**(a) indicates the runoff of water stored in the catchment before the event while other partitioned constituents (1~4) are generated by the rainfall during the event. Additionally, how to partitioning hydrograph spatially with respect to 6 subcatchments (A~F) is shown in **Fig. 3**(b). Spatial separation allows the hydrologists to discriminate between dominant and non-dominant sub-units of catchment at each time step whence provides a useful information on water sources and pathways that are often required in order to examine ecological issues like a hydrological effects of ecosystem disturbance.

The spatiotemporal record matrix as illustrated in **Fig. 3**(c) is employed so as to track where streamflow comes from when it rains. The dimensions of matrix, $\boldsymbol{R}_i(t)$ are given with $\boldsymbol{S}$ rows, number of sub-units within catchment and $\boldsymbol{T}$ columns, number of temporal classes where i is a subcatchment and t is time. **Fig. 3**(c) shows the spatiotemporal matrix at time t at the outlet, for example, the value belonging to spatial zone C and temporal class 2 implies that the proportion of runoff in (C,2) entry to the stremflow observation at time t is 6%. As summarizing whole values vertically along the columns, we can obtain the information, temporal contribution of rainfall to streamflow. Likewise, the spatial influence of subcatchments on streamflow can be assessed by horizontal summation along the rows. As a result, we readily distinguish between old water (*i.e.* pre-event water at time class 0 possesses 15%) and new water (*i.e.* new water components are 30% at time class 1 and 55% at time class 2, respectively)

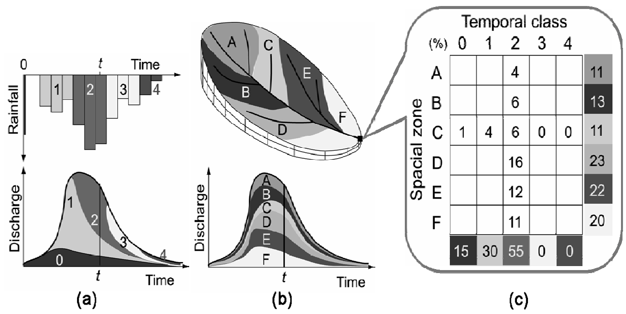

Fig. 3 Schematic diagram of hydrograph separation based on (a) temporal record of streamflow, (b) spatial record of streamflow and (c) spatiotemporal record matrix of streamflow (Sayama *et al*., 2007); $\boldsymbol{S}$=6, $\boldsymbol{T}$=5.

at the target time t. Moreover, it is possible to track the spatially distributed origin for streamflow generation, for instance, downstream spatial zones (*e.g.* D, E and F) contribute more than 60% of streamflow whereas upstream classess (*e.g.* A, B and C) less affect streamflow generation at time t.

5. CASE STUDY

The study site is the Kamishiiba catchment, upstream area of the Kamishiiba dam, which lies within Kyusu region in Japan and covers area of 211km^2 (see **Fig. 5**(a)). The topography of this area is hilly with the elevation varying from 400m to 1700m. Most of land use type is forest, thereby can be regarded as typical Japanese mountainous area. In the model, catchment is represented by 250m×250m DEM. The observed discharge data converted from water level of dam inflow having 10min temporal resolution is available. To show the clear performance of old water, occurred during pre-event, with respect to plausible parameter combinations, we select a sufficiently long historical event (192hours).

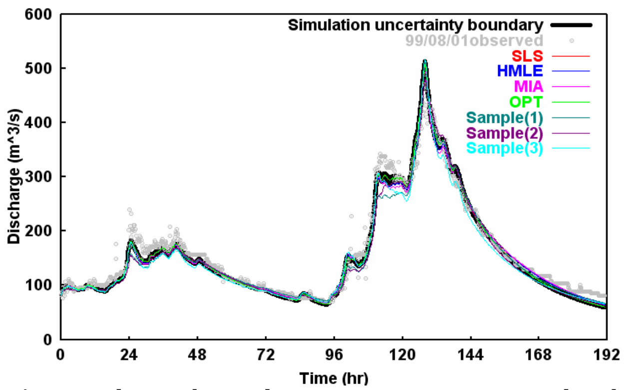

Fig. 4 Hydrograph simulation uncertainty associated with the behavioral parameter sets (*i.e.* 5400 (=6000×90%) hydrographs are plotted) derived using the SCEM and simulated hydrographs associated with plausible parameter sets.

1) Global response of catchment and propagation of parameter uncertainty

Probabilistic results of the hydrograph are obtained from the ensemble simulation of OHDIS-KWMSS for 6000 parameter sets sampled from the posterior parameter distribution. **Fig. 4** shows how the parameter uncertainty propagates into estimates of hydrograph simulation uncertainty. Moreover, the reproduced hydrographs with respect to plausible parameter sets are included in **Fig. 4**. In this figure, the light grey dots indicate the observed streamflow data and the black shaded region is 90% hydrograph simulation uncertainty associated with the posterior distribution of the parameter estimates.

In spite of considerable parameter uncertainty (*i.e.* unknown initial parameter uncertainty range is reduced to constrained boundary through SCEM trials, see **Fig. 2**(f)), the resultant boundary of hydrographs are very narrow. It can be interpreted that complex rainfall-runoff model is likely to be exposed to equifinality problem so that it makes difficult to discriminate quantitatively and qualitatively between reliable and unreliable parameter sets. Moreover, it supports the fact that only streamflow data is not sufficient to identify model parameters precisely.

Indeed, as shown in **Table 1** and **Fig. 4**, all of parameter sets used here lead to considerably similar outputs in terms of quantity (*i.e.* Nash-Sutcliffe Efficiency values of all hydrographs are more than 0.95) and quality (*i.e.* visual goodness-of-fit between the observed and simulated hydrographs). Therefore, the complementary constraint is necessary to augment power to select the erroneous parameter combination(s) out from a large number of plausible ones. In many hydrological questions, it may be much more interest to know what happens inside a catchment than at the outlet. The subsequent subsections demonstrate the internal dynamic response of catchment to these plausible parameter sets.

2) Spatially distributed origins for plausible parameter sets

The study catchment is represented by 3190 rectangular slopes (*i.e.* ***S***=3190) and contributions of each slope to each streamflow observation at selected time steps, 1, 48, 134 and 182 hours are illustrated in Figure 5(a). At the beginning of rainfall-runoff process (*e.g.* 1hour), the adjacent slopes to river channel, referred to as riparian zone constitute primarily the streamflow while water stored in other upstream slopes do not reach to the river yet. As time goes on, contributive slopes spread gradually from near to far and eventually, all of slopes influence on streamflow generation. The contribution of each slope to streamflow is represented by Relative Ratio of Total Discharge (RRTD) at the specific time step, defined as:

$$\mathrm{RRTD}_i(t) = \frac{D_i(t)}{D^{outlet}(t)} \times 100 \quad (\%) \qquad \sum_{i=1}^{S} \mathrm{RRTD}_i(t) = 100 \quad (\%) \tag{3}$$

where i is slope number and $D_i(t)$ is discharge at the outlet from slope i within catchment at time t. $D^{outlet}(t)$ is total discharge of the outlet at time t. Each RRTD for specific four time steps is categorized into eight classes as shown in **Fig. 5**(a). Colorful snapshots for spatially distributed origin apparently present that even though global responses of catchment with respect to the plausible parameter sets are nearly identical, the internal responses are completely different.

The variations of spatial origin for the different parameter sets are summarized by two indices. First, how many slopes are included in each RRTD class is represented by Relative Frequency of Slope (RFS) index:

$$\mathrm{RFS}_j(t) = \frac{N_j(t)}{\boldsymbol{S}}, \qquad \sum_{j=1}^{8} \mathrm{RFS}_j(t) = 1 \tag{4}$$

where $N_j(t)$ is the number of slopes included in RRTD class j at time t, S is the total number of slopes.

Secondly, how much each RRTD class contributes to generate streamflow observations is quantified by Ratio of Contribution to Streamflow Generation (RCSG) index:

$$\mathrm{RCSG}_j(t) = \sum_{i \in j} \mathrm{RRTD}_j(t) \qquad \sum_{j=1}^{8} \mathrm{RCSG}_j(t) = 100 \quad (\%) \tag{5}$$

All of values for the RFS and RCSG are plotted in **Fig. 5**(b). The number of slopes in RRTD class 3 for Sample(1) and (2) is larger than others at the beginning of runoff but the level of their contribution to streamflow is very similar (see the RCSG at the 1hr). It supports that even if the locations of origin are different, the equivalent amount of streamflow can arise from those. At the

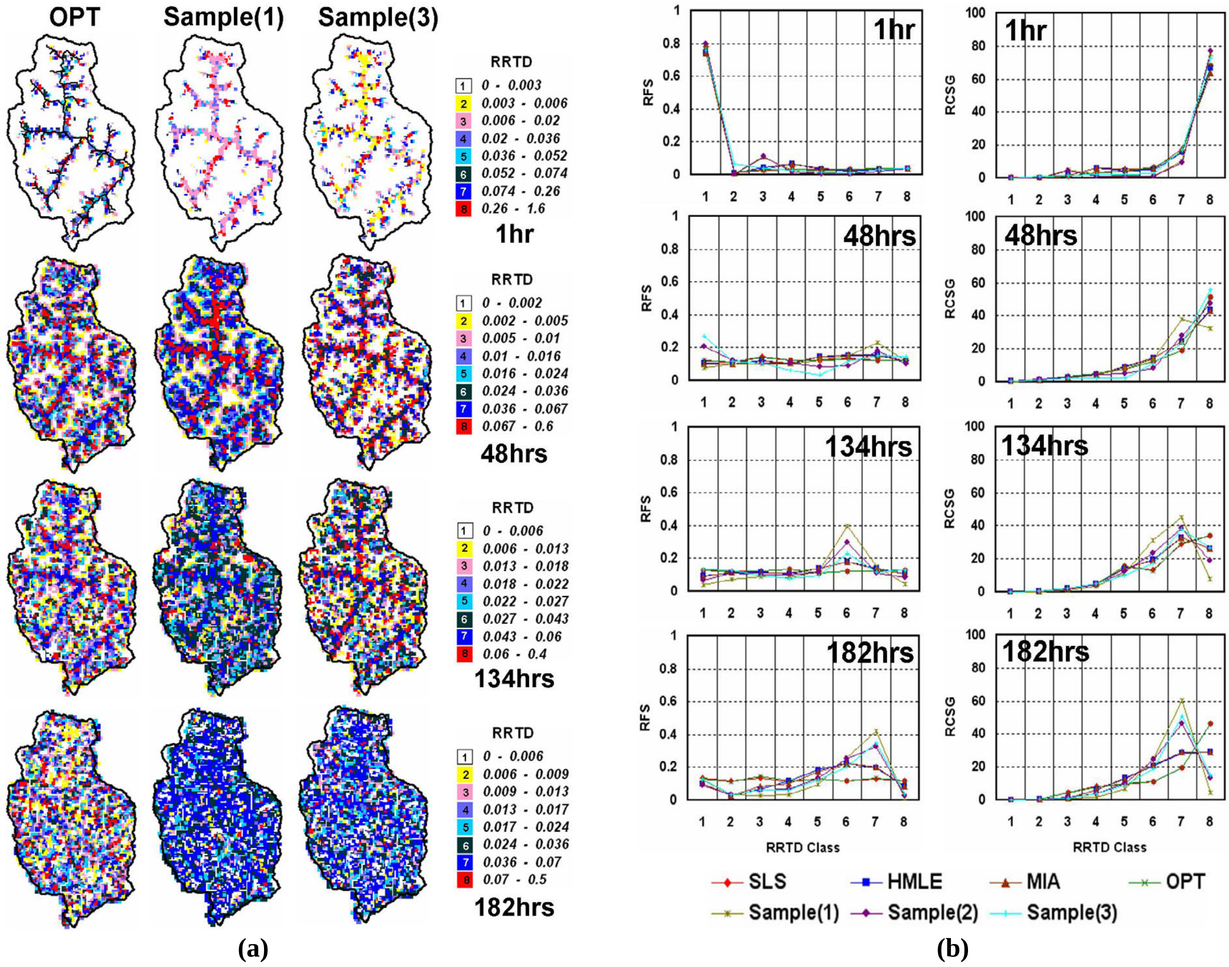

Fig. 5 (a) Spatially distributed origins of streamflow for OPT (note that channel network is plotted as black solid line only in the left top snapshot for OPT at 1hour), Sample(1) and Sample(3) at time 1, 48, 134, 182 hours (b) RFS and RCSG for the selected four time steps.

48hour, both RFS and RCSG show relatively the balanced results (*i.e.* all of slopes contribute to streamflow while their amounts of contribution are different according to parameter sets). Furthermore, the internal response of catchment in terms of RFS and RCSG obviously show the different patterns as the catchment becomes sufficiently saturated, for example, Sample (1) ~ (3) at 134 and 182 hours are more deviated, especially, in RRTD classes 6~8, as compared with other cases. Interesting finding is that the parameter sets for SLS and OPT provide similar results in spite of marginal difference between the values of two parameter sets. It means that these two plausible sets should be retained for model prediction unless and until additional evidence to the contrary becomes apparent because even auxiliary information used here cannot constrain the model completely.

3) Temporally separated components of stream flow for plausible parameter sets

The study event is split into six temporal classes (*i.e.* ***T***=6; pre-event, 0~25hrs, 26~96hrs, 97~109hrs, 110~120hrs and 121~192hrs) and then the simulated hydrographs are separated into corresponding six components by using temporal record of the proposed matrix. In the same manner, temporally separated constituents with respect to different parameter values yield different aspects. In Sample (1) ~ (3) cases, old water posses more than 50% of streamflow while they are approximate 40% in OPT and SLS cases and less than 35% in HMLE and MIA cases, respectively (see **Fig. 6**).

The corresponding amount of each hydrograph component to selected six rainfall segments is summarized in **Table 2**. As well as overall behavior in terms of the simulated hydrograph and the variation of spatial origin of streamflow above demonstrated, the temporal components with respect to SLS and OPT parameter sets provide similar results in spite of nominal difference in terms of three parameters, d_s, d_c and β. However, other components vary differently owing to different conceptual parameter related with subsurface flow.

From the application results, it can be seen that a complex distributed rainfall-runoff model can permit multiple alternative spatiotemporal flow pathways for rainfall over catchment to transform into runoff and the commonly used streamflow data to evaluate such model does not contain any inform-

Table 2 Summary of temporally-separated components of the simulated hydrographs.

Temporal Class / Sample	Old Water (%)	New Water (%)				
		1	2	3	4	5
SLS	40	9	13	11	12	15
HMLE	34	12	15	12	12	15
MIA	32	13	15	13	12	15
OPT	40	9	13	11	12	15
Sample(1)	54	11	10	9	8	8
Sample(2)	56	9	10	7	8	10
Sample(3)	59	7	8	7	8	11

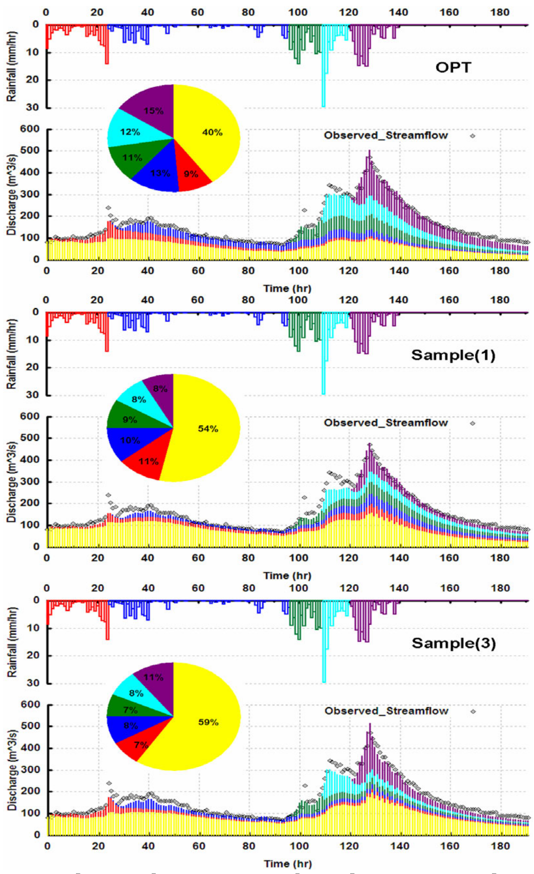

Fig. 6 Hydrograph separation based on temporal record of streamflow for OPT, Sample(1) and Sample(3).

ation on these possible pathways. As a result, if additional comparable observed data is available, the proposed information in terms of the spatio temporal internal behavior of catchment can be utilized as complementary evaluative criterion to filter out unreliable parameter set(s).

6. CONCLUSION

This paper addressed the limitation of streamflow data to identify the most reliable parameter set and the necessity of complementary constraint to select the unreliable one out from numerous plausible parameter combinations. The spatiotemporal record matrix of streamflow was applied to the nonlinear distributed rainfall-runoff model, OHDIS-KWMSS in order to investigate the global and internal dynamic responses of catchment with respect to seven plausible parameter sets. Summarized results from this study are as follows:

1) The behavioral parameter sets provide similar results in terms of OFs and simulated hydrographs even though they have different values.
2) It is possible to separate spatiotemporally hydro graph of a mesoscaled catchment and this result would be comparable with the separated hydrograph by using observable hydrochemical measures.
3) Spatiotemporal internal response of catchment provides new information capable of narrowing down more physical and reliable range of parameter set(s).

It is concluded that the incorporation of the complementary constraint into evaluation procedure can be a more advanced approach to solve equifinality problem than the utilization of only streamflow data.

REFERENCES

1) Duan, Q., Sorooshian, S. and Gupta, V.K.: Effective and efficient global optimization for conceptual rainfall-runoff models, *Water Resour. Res.*, Vol.28, No.4, 1015-1031, 1992.
2) Beven, K.: Prophecy, reality and uncertainty in distributed hydrological modeling, *Adv. Water Res.*, Vol.16, No.1,, 41-51, 1993.
3) Beven, K. and Binley, A.M.: The future of distributed models: model calibration and uncertainty prediction, *Hydrol. Processes*, 6(3), 279-298, 1992.
4) Kuczera, G. and Franks, S.W.: Testing hydrologic models: Fortification or Falsification?, in *Mathematical Models of Large Watershed Hydrology*, edited by V. P. Singh, and D. Frevert, pp. 141-185, Water Resources Publishers, Highland Ranch, Colorado, 2002.
5) Mroczkowski, M., Raper, G.P. and Kuczera, G.: The quest for more powerful validation of conceptual catchment models, *Water Resour. Res.*, Vol.33, No.10, 2325-2336, 1997.
6) Franks, S.W., Uhlenbrook, S. and Etchevers, P.: Hydrological simulation, in *Hydrology 2020: An integrating Science to Meet World Water Challenges*, IAHS Publ. 300, edited by T. Oki, Valeo, C. and Heal, K., pp. 105-122, IAHS Press, Wallingford, 2006.
7) Kirchner, J.W.: Getting the right answers for the right reasons: Linking measurements, analyses, and models to advance the science of hydrology, *Water Resour. Res.*, Vol.42, W03S04, doi:10.1029/2005WR004362, 2006.
8) Sayama, T., Tatsumi, K., Tachikawa, Y. and Takara, K.: Hydrograph separation based on spatiotemporal record of streamflow in a distributed rainfall-runoff model, *J. Japan Society of Hydrol. & Water Resours.*, JSCE, Vol.20, No.3, 214-225, 2007.
9) Tachikawa, Y., Nagatani, G. and Takara, K.: Development of stage-discharge relationship equation incorporating saturated–unsaturated flow mechanism, *Annual J. Hydraul. Eng.*, JSCE, Vol.48, 7-12, 2004.
10) Lee, G., Tachikawa, Y. and Takara, K.: Identification of model structural stability through comparison of hydrologic models, *Annual J. Hydraul. Eng.*, JSCE, Vol.51, 49-54, 2007.
11) Vrugt, J.A., Gupta, H.V., Bouten, W. and Sorooshian, S.: A shuffled complex evolution metropolis algorithm for optimization and uncertainty assessment of hydrologic model parameters, *Water Resour. Res.*, Vol.39, No.8, 1201, doi:10.1029/2002WR001642, 2003.

(Received September 30, 2007)